Journal of Autonomous Intelligence (2024) Volume 7 Issue 1
doi: 10.32629/jai.v7i1.749

ORIGINAL RESEARCH ARTICLE

Combined deep learning and machine learning models for the prediction of stages of melanoma

Rashmi Ashtagi[1,*], Deepak Mane[1], Mahendra Deore[2], Jyoti R. Maranur[3], Sridevi Hosmani[3]

[1] *Department of Computer Engineering, Vishwakarma Institute of Technology, Bibwewadi, Pune 411037, India*

[2] *Department of Computer Engineering, MKSSS's Cummins College of Engineering for Women, Karve Nagar, Pune 411052, India*

[3] *Faculty of Engineering and Technology (Exclusively for Women), Sharnbasva University, Kalaburagi 585103, India*

*** Corresponding author:** Rashmi Ashtagi, rashmiashtagi@gmail.com

ABSTRACT

Melanoma is deadly kind of skin cancer as it gets metastasized soon. It is really essential to recognize melanoma and start treatment at early stage. It is also necessary to determine the stage of melanoma in order to treat melanoma patients. Non-invasive technique is required to detect the stage of melanoma. Proposed system presents novel technique to classify the stages of melanoma based on thickness of tumor. This system uses dimensionality reduction technique to reduce the number of features and it also uses combine approach of deep learning (DL) and machine learning (ML) algorithm which include multilayer perception (MLP) and random forest (RF). Deep learning method is always better for training as they can reduce the need for data preprocessing and feature engineering and can provide simple trainable models built using only five or six different operations. Secondly, they are scalable, as they can be easily parallelized on GPUs or TPUs and can be trained by iterating over small batches of data. Thirdly they are reusable, so they can be trained on additional data without starting from scratch, making them viable for continuous online learning. For classification task machine learning algorithm that is, random forest is used as it decreases over fitting in decision trees and aids to increase the accuracy. Total of three algorithms were used, MLP, RF and proposed algorithm combined multilayer perception and random forest that is, MLP-RF. Among these models, the MLP-RF showed the best results in predicting melanoma stages with the accuracy of 97.42%.

Keywords: deep learning; dimension reduction; random forest; multilayer perception; stage of melanoma

ARTICLE INFO

Received: 19 June 2023
Accepted: 12 September 2023
Available online: 27 October 2023

1. Introduction

The skin, being the body's most important and largest organ, protects us from sunlight, heat, certain sun's harmful rays, infections, and wounds. Skin has an important role in storing water, vitamin D, and fat, as well as maintaining internal heat levels. Most perilous type of skin cancer is malignant growth. Malignant development is created as not repaired DNA harm to skin cells and for the most part it is realized by radiation from sunshine and furthermore as a result of hereditary deformities. It is brought about by burns from the sun brought about by ultraviolet rays. Melanoma is the fatal kind of skin cancer. It resembles moles and might have been formed by moles. Melanomas can be brown, black, purple, skin-colored, red, pink, white, or blue in color. However, the likelihood of a black or brown color is greater. In the event that melanoma is detected and treatment started at beginning period, it can be cured. The malignant development can

proceed and spread to various parts of body, and it ends up being difficult to cure and can be deadly[1,2].

Dermoscopy is non-invasive technique utilised to look at skin lesion. Dermoscopy is extra exact compared to exposed eye assessment for investigation of cutaneous melanoma. There are numerous strategies to identify melanoma or favorable from dermoscopic pictures[3].

Melanoma metastasizes quickly in most cases. As a result, clinicians should identify and diagnose melanoma at its early stage, when odds of cancer having already metastasized are lower and the survival chances are higher. For detecting stage of melanoma thickness is measured for that Breslow index is used. Because of the minimal difference between enclosing lesions and skin, visual similarity amongst lesions, confusing boundaries of lesions, and so on, skin lesion prediction from a dermoscopic picture is a challenging job in any case, even for expert dermatologists. With provided dermoscopic images, an automated computer-aided detection method can assist physicians in predicting the prognosis of malignant skin lesions at an early stage. Expanded convolution, which has increased exactness with a same amount of computing complexity when compared to deep learning algorithms, is a current breakthrough in deep learning. Finding of an obscure skin lesion is essential to empower appropriate medicines.

Breslow index

Using an ocular micrometre, the Breslow Index calculates the maximum thickness of a skin lesion by measuring it from the top of the granular cell layer to the deepest point of infiltration. This measurement takes place from the center of the lesion outward. If the skin lesion is already ulcerated, the ulcer base that is above the deepest point of invasion is what is used for diagnosis and treatment rather than the top of the granular cell layer[4]. For the purposes of pathological analysis, a suspected skin lesion can be obtained through either an incisional or an excisional biopsy. Incisional biopsy is a technique for determining the composition of a skin lesion by removing a small piece of tissue. Excisional biopsy is a technique that involves removing the whole suspicious skin lesion. To determine the risk of advancement, the thickness of the melanoma must be measured prior to surgical removal. The inaccuracy of tumour size in predicting prognosis might be attributed to merely examining size in two dimensions; tumour volume must also be taken into account. Although 2 melanomas skin lesions can have same diameter, their thickness might vary substantially. If the width and thickness of the melanoma are the same, the stage of the cancer will be different[5].

Ashfaq A. Marghoob et al. categorised tumour thickness into 4 categories: thickness ≥ 0.75 mm, thickness 0.76–1.5 mm, thickness 1.54–4.0 mm, and thickness > 4.0 mm. Their outcome show that level is a significant independent variable for thin melanomas and all other thickness categories[6]. The stages of melanoma and their thickness values are shown in **Figure 1**. Melanoma that has reached stage 0 is known as situ melanoma. The cancer cells in melanoma at this stage are contained to the epidermis and have not yet begun to invade deeper layers of skin. The thickness of melanoma in stage IA is less than 0.75 mm. There are no wounds or ulcers in the skin layer that covers the tumour. Melanoma in stage IB that is 0.76 to 1.5 mm thick. There has been no spread to any other bodily parts; it only affects the skin. Melanoma may develop ulcerated if it has progressed to stage II. Under a microscope, stage IIIA melanoma can be shown to have spread to up to 3 nearby lymph nodes. Stage IIIB melanoma has advanced to lymph nodes that are inflamed and ulcerated. Stage IV melanoma has spread.

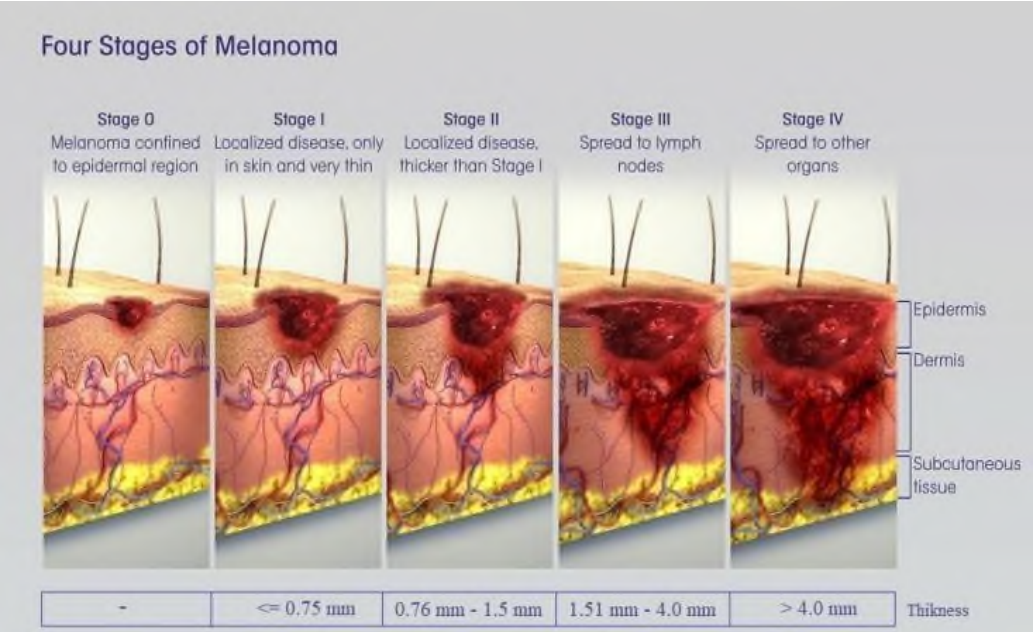

Figure 1. Stages of melanoma and their thickness values.

Early detection of melanoma considerably raises survival rate. Only highly trained dermatologists are capable of correctly identifying melanoma skin lesions based on a dermoscopic image of the lesion. Nonetheless, because of the tiny difference amongst skin and lesion, visual similarity between melanoma and benign, and other factors, precisely identifying melanoma is very difficult. As a result, non-invasive techniques are necessary to distinguish between melanoma and benign. Overall, a new technique to cope with obstacles for exactness and automated melanoma stage diagnosis in the HAM10000 dataset was developed to address these concerns. Melanoma stage detection frameworks are being developed. We also used cloud computing services to speed up the process and protect sensitive user data including sickness information. MLP is utilised for training and RF is used for classification in the first system. The MLP is good for training datasets, whereas RF is good for classification since it is broader. The primary benefit of RF is that it provides a consistent framework within that various learning machine models may be built by correct chunk selection. Advantages of both MLP and RF are considered and novel framework is designed which is combination of MLP and RF as MLP-RF. In second framework, Dimensionality reduction is performed using t-SNE algorithm which reduces number of features from dataset and then updated dataset is pass to Hybrid classification algorithm (MLP-RF), this gives more accuracy and sensitivity compared to other systems. Following **Table 1** shows the various objective and research question related to melanoma stage detection.

Table 1. Research question and answer.

Research question statement	**Answer of questions**
Which deep learning-based classifiers are utilised to diagnose melanoma stage?	Multi-Layer Perceptron.
What difficulties and possibilities do deep learning algorithms for melanoma stage detection present?	Deep Learning model alone gives less accuracy.
What performance measures do classification techniques employ to diagnose melanoma stage?	Accuracy, Precision, Recall, F-score.
What are the classifiers' accuracies?	MLP-87.3%, RF-91.1%, MLP-RF-91.8%. MLP-90.54%, RF-91.89%, MLP-RF-96.77% (with dimension reduction algorithm).
What kinds of datasets are accessible for melanoma stages diagnosis?	Only single dataset is available
What are steps utilised to improve performance of system?	Proposed MLP-RF with dimension reduction.

We included information from all studies in Section II (Literature Survey). The current architecture of proposed system is presented in 3rd section. Experimental setup and dataset utilised are explained in 4th section. Conclusion and future effort necessary to enhance our system were mentioned in section 5 (Conclusion).

2. Literature review

Using dermoscopic images, there are a variety of ways for distinguishing melanoma from benign tumours. It's crucial to determine the melanoma stage by looking at thickness of the tumour on dermoscopic images. The use of noninvasive methods to determine the type or stage of melanoma receives very little attention. The stage of cancer determines the patient's prognosis.

Patil and Bellary[7] suggested two techniques for melanoma cancer stage classification. According to first method, melanoma is divided into two stages: stage 1 and stage 2. Melanoma is divided into three phases according to the second classification system: 1, 2, and 3. The proposed solution makes use of a convolutional neural network that has Similarity Measure for Text Processing as its loss function. Sáez et al.[8] offered system for determining the thickness of melanoma using dermocospic images. There were two supervised categorization systems suggested. The first method divides melanoma into two categories: thin and thick. Binary categorization differentiates between thin and thick melanomas. In second method, it is divided into three categories: thick, thin, and intermediate. The LIPU model of logistic regression employs both logistic regression and neural networks. It continues to be remarkably accurate. The results demonstrates that the LIPU model accurately predicts outcomes for both two-class and three-class variations of the problem. Rubegni et al.[9] presented a method that divides tumours into thick and thin melanomas depending on thickness of melanoma. The digital dermoscopy analysis incorporates software to allow for computerised examination of images and the research of morphological characteristics of lesions. Melanoma pictures were evaluated for 49 distinct qualities, including colour, structure, and texture, as well as their integration. There were 141 melanoma images utilised, with an accuracy rate of 86.5 percent. Thin melanomas accounted for 97 of the 108 cases, whereas thick melanomas accounted for 25 of the 33 cases. Jaworek-Korjakowska et al.[10] presented a method that uses tumour thickness to determine the stage of melanoma cancer. The VGG16 CNN is used for transfer learning. With an accuracy of 87.2 %, this method can classify melanoma into three phases. A. Naeem et al. presented deep learning on melanoma classification[11]. According to their findings, CNN-based classifiers recognise skin cancer pictures as well as dermatologists, allowing for a rapid and life-saving diagnosis. Additionally, a thorough analysis of the most current studies on CNN-based melanoma categorization is included in their research. They exclusively focused on binary categorization of melanoma in their research. They completed a total of 5112 studies, of which 55 were chosen for further investigation.

Reshma and Shan[12] presented a technique for determining melanoma stage based on overall dermoscopic score. The image is preprocessed with rgb2gray conversion and a median filter to decrease noise. The edge detection technique Sobel is used. Patil and Bellary[13] and Gaikwad et al.[14] propose techniques to identify melanoma from benign. They also identified type of melanoma is identified by using different transfer learning techniques[15]. Then, they presented grouping of CNN and SVM approach for melanoma and benign categorization from ISIC2017 dataset[16].

Ichim and Popescu[17] proposed novel neural networks approach linked on 2 classification phases. This method facilitates system's transfer from one database to another. A cost-effective approach was proposed for melanoma identification in lesion images using several classifiers. Following considerations were taken into consideration when picking classifiers: a) Two hierarchical tiers of classifiers will be used: one subjective and one objective b) First stage classifier to use various lesion characteristics c) Relevant learning found any classification dependent on characteristics to be subjective, and d) Inclusion of a final classifier. Implementation of a conditional GAN for classifying accidents based on the ABCD law was also a key addition to this. The precision of the classifier was improved. The TDS score was converted into probability to be

associated with the final classifier. The benefit of the planned two-tier framework was to switch between databases (or devices) quicker, only learning the second stage. System suggested improves efficiency of other comparison methods. Therefore, the neural network reaches 97.5% ACC and 94.47% F-score, respectively.

Saleh Albahli et al.[18] published a study in which they presented a melanoma detection and segmentation method. By applying morphological operations to the dermoscopic images, artefacts such as gel bubbles, clinical marks, and hairs are removed, and image regions are sharpened. They employed the YOLOv4 object detector, which was optimised for melanoma identification, to distinguish between strongly correlated infected and non-infected areas for infected region detection. On the ISIC2018 and ISIC2016 datasets, the suggested method is tested, and the results proved more efficiency comparatively.

Using an ideal CNN, Zhang et al.[19] described a novel image processing-based approach for early diagnosis of skin cancer. The suggested approach's performance was evaluated using two distinct benchmarks, Dermquest and DermIS, and outcomes were compared to ten other approaches, such as semi-supervised technique, Spot-mole tool, Ordinary CNN, AlexNet, VGG-16, Inception-v3, and ResNet. Specificity, Acc, sensitivity, and precision are the performance indicators used here.

Kassem et al.[20] presented an approach utilizing the transference learning and pre-trained Google Network was developed for ISIC 2019 Challenges Data Set. Eight different types of lesions can be precisely classified in the proposed method, even with imbalances between categories. The performance of suggested technique improved when each class images number was decreased to solve unbalanced problem between classes. When weight is adjusted for all architecture layers, performing measures are greater than just the finished layers. Only the replaced layers are finished. A different model suggested that unknown images be detected via GoogleNet and SVM multi-class systems. The authors tried to use the VGG19 as they used GoogleNet, but could not use or test the same equipment. It calls for specific hardware specifications which all researchers in various countries cannot fulfil.

Cirrincione et al.[21] proposes a ViT-based architecture that can distinguish between lesions that are malignant and non-cancerous is given. The ISIC challenge's public skin cancer data is used to train and test the suggested prediction model, and the results are very encouraging. The best discriminating classifier configuration is chosen after careful consideration and analysis of many configurations. The best one achieved 0.948 accuracy, 0.928 sensitivity, 0.967 specificity, and 0.948 AUROC.

3. Proposed system

In **Figure 2** shows the proposed system architecture which takes melanoma stages dataset as input. Data cleaning and data normalization steps are performed after reading dataset. The normalized data is pass to dimensionality reduction as dataset contains 81 attributed[8]. Dimensionality reduction using t-SNE is also performed to reduce the number of features. After reducing features 80% training and 20% testing dataset are split and it pass classification algorithm where 10-fold cross validation is performed. In classification MLP, RF and proposed algorithm MLP-RF is used. After performing classification stages of melanoma are detected as stages 1, 2 and 3. At end performance evaluation is done on the basis of accuracy, recall, precision, and F-measure.

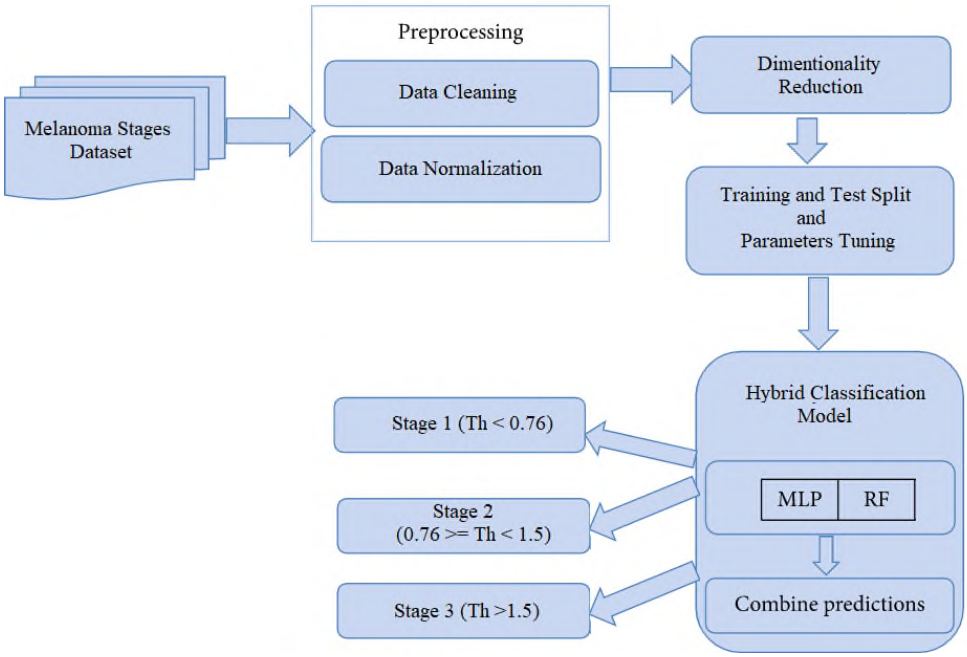

Figure 2. Proposed system architecture.

3.1. Supervised-learning

In order to correctly model the data, certain algorithms require normalization. Assume two columns in the input dataset, one from 0 to 1, and the other from 10,000 to 100,000. Values with a wide range of magnitudes may be challenging to represent as features, hence we have normalized data with wide range of magnitudes. The normalizing formula is as follows:

$$X' = \frac{X - X_{min}}{X_{max} - X_{min}} \quad (1)$$

X_{max} and X_{min} denote highest and lowest values of a feature.

When the value of X is equal to or lower than the minimum value of the column, the numerator will be 0, and X' will also be 0.

When the value of X is the highest in the column, the numerator and the denominator will be equal; hence, X' will be equal to 1.

The value of X' swings between 0 and 1 if value of X falls between lowest and maximum

3.2. Features used

The characteristics that are utilised to classify melanomas are given in this section. The extraction is based on results from clinical trials that show a link between specific features detected in dermoscopic images and melanoma thickness. Dermoscopic structures and color characteristics are the focus of these results. Color, and texture are used to extract a total of 81 descriptors (x1–x81). The following features are taken from an image dataset, and a new dataset is made and saved as a CSV file.

- Shape features
- Color feature
- Pigment network features
- Texture features

3.3. Dimensionality reduction

When dealing with classification issues, there are generally an excessive number of characteristics upon which to base the ultimate category. Basically, these components are traits, which are variables. More features

there are, the harder it is to imagine a train set and a test set on it. The majority of the traits are often connected and hence redundant. In this case, dimensionality reduction methods are beneficial.

3.4. Dimensionality reduction advantages

- It facilitates data compression, which reduces storage requirements and computation time.
- It also aids in the removal of redundant features if any exist.

3.5. Working of t-distributed stochastic neighbor embedding (t-SNE)

An approach starts by estimating likelihood of points in high-dimensional space and low-dimensional space being comparable.

A point's conditional probability of picking a neighbor is used to determine point similarity. SNE uses a gradient descent technique to limit the total Kullback-Leibler divergence of all the data points, which is a way of measuring how much the total difference in conditional probability is minimized.

By measuring pairwise similarities of input objects and low-dimensional points in embedding, t-SNE lowers the divergence between the two distributions. Aiming to uncover patterns in data by mapping multi-dimensional data to a lower-dimensional space and comparing data points with diverse attributes. Input characteristics are no longer recognizable after this procedure, and you can't make any inferences based only on the t-SNE output. As a result, it's mostly a data exploration and visualization method.

3.6. Random forest (RF)

This is well-known ML technique is a subset of supervised learning algorithm and can be implemented in a variety of ways. It can utilize in ML for classification and regression. It is based on the concept of combining a large number of classifiers in order to address a difficult issue and enhance model performance. Its name implies that it "combines a large number of decision trees on distinct subsets of a given dataset and averages their prediction performance". Random forest is a method for predicting outcomes that does not rely on a single decision tree but rather takes into account the votes from all of the trees together. The more trees in the forest, the more exact it is, avoiding overfitting. This well-known machine learning approach is a subset of the supervised learning algorithm. It may be utilised in both classification and regression. A model's performance may be improved by combining several classifiers. The random forest is constructed by combining N different decision trees, and then generating predictions for each individual tree that was formed in the initial phase.

Phases in working process are outlined below, and **Figure 3** depicts the procedure:

1) From the training set, pick K data points at random.

2) Make decision trees for data points selected.

3) Choose N as the number of required decision trees to be constructed

4) Steps 1 and 2 should be repeated.

5) Find the forecasts for new data points in each decision tree, and then place those new data points in the category that received the most votes.

$$X = x_1, x_2, \ldots . x_n \tag{2}$$

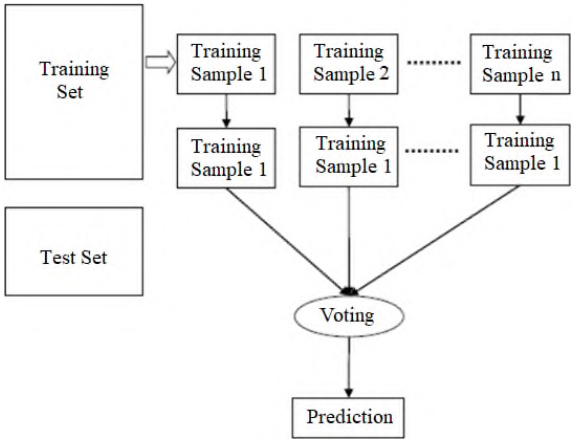

Figure 3. Random forest algorithm working.

3.7. Multi-layer preceptor (MLP)

The MLP is associated with the formation of tightly linked neurons that connects adjacent layers as shown in **Figure 4**. The contribution through one layer has never been passed back to the earlier layers in Feed Forward Neural Networks, which is one of their peculiarities. The weighted average is the input to each neuron from the previous neural network layer's outputs. This input is translated into output via a consistent and separable activation function. The output is created after the signals have travelled from input layer to output layer. Pass error is calculated; for regression, correlation coefficient or mean squared error is commonly utilised. To reduce error, the supervised learning, which is basically a back propagation algorithm, calculates the gradient of the neurons as required. Until the specified number of iterations is reached, the data is passed to the framework numerous times such that the parameters can be changed to reduce the errors.

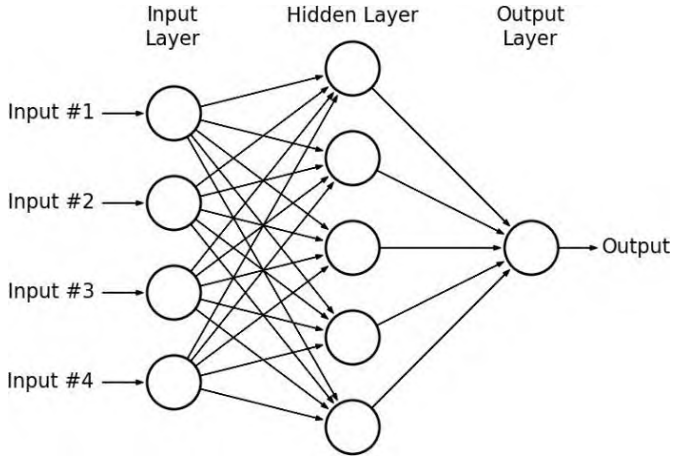

Figure 4. Working of multilayer perceptron.

3.8. MLP-RF

As shown in **Figure 5**, MLP and RF were developed to be trained with the image set. For the development and training of the MLP and RF, the Tensor Flow package and keras subclass were used. Three tf.keras. layers dense can be found in the MLP. A tf.keras was given dense layers, which are conventional concealed layers. Sequential model with 128 nodes in first layer, 12 nodes in second layer, and a final output node. The first two levels utilised max(0, t), where t is a node's value. The last layer uses multiclass classification softmax activation function. The tf.keras.Model. Compile method then trains model on training set.

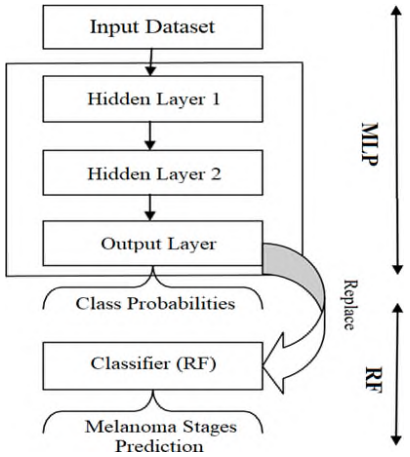

Figure 5. Represents the proposed hybrid classifier MLP-RF.

Loss function utilised in model fitting was a cross-entropy, which is

$$L(y) = -\frac{1}{N}\sum_{i=1}^{N} y_i \log(p(y_i) + (1 - y_i)\log(p(1 - y_i)) \quad (3)$$

where *y* is the output vector.

The method of optimization is gradient descent,

$$w = w - a(\delta loss/\delta w) \quad (4)$$

where *w* is the weight and a is a learning rate. Because previous experiments with higher learning rates resulted in more fluctuation in accuracy across epochs, the learning rate used was 0.001. With the training set, this model would be trained for 500 epochs. Last but not least, the model's findings were recorded and shown using matplotlib and the sklearn module, including accuracy, loss, and receiver operating characteristic (ROC) curve. For Random Forest, sklearn.ensemble function is used, and number of estimators is set to 100.

4. Results and discussion

4.1. Dataset description

Experiments are carried out using melanoma dataset[8], which may be downloaded at https://www.uco.es/grupos/ayrna/ieeet-mi2015. There are 81 characteristics in dataset, which is divided into binary and multi-class datasets. There are 250 images of melanoma cancer in total: 167 melanomas with a thickness < 0.76 mm, 54 melanomas with a thickness 0.76–1.5 mm, and 29 melanomas with a thickness greater than 1.5 mm. These pictures' extracted characteristics were utilised. These images have 81 characteristics extracted from them.

4.2. Experimental setup

The prediction models proposed in this paper are implemented on the Windows 10 Professional platform. It can be performed on a computer with 500 GB SSD and 8 GB of RAM. Models' implementation code was written in Python 3.7 and above using the anaconda (Jupiter notebook) development environment. The technique used in the prediction model are RF, MLP and proposed algorithm MLP-RF.

4.3. Performance analysis

The robustness of this approach is evaluated using metrics listed below. Generally accurate It is determined as the percentage of labels that have been properly identified across samples from all classes. TP, TN, FP, and FN, respectively, represent the number of true positives, true negatives, false positives, and false negatives.

$$Accuracy = \frac{(TP + TN)}{(TP + TN + FP + FN)} \tag{5}$$

$$Recall = \frac{TP}{(TP + FN)} \tag{6}$$

$$Precision = \frac{TP}{(TP + FP)} \tag{7}$$

$$F - score = \frac{(2 \times TP)}{(2 \times TP + FP + FN)} \tag{8}$$

4.4. Result analysis

Accuracy measure is utilised to compare performance of approaches on a quantitative and qualitative level. Based on the methods and approaches employed, the comparative research is separated into two groups. In the first group, the suggested method's performance is compared to that of various machine learning methods. The performance of the suggested approach with features dimensionality reduction is compared to the performance of the ML methods in the second group. As Dataset Size is less data augmentation is performed. The obtained results of the first group are demonstrated in **Table 2** while respective graph is demonstrated in **Figure 6**. And the second group results are demonstrated in **Table 3** and its respective graph is demonstrated in **Figure 7** Various parameters of proposed MLP-RF approach including recall, precision, F-score and accuracy are compared with RF, MLP. Our results outperform the other methods in most of evaluation metrics. There is significant increase in precision, recall, F-score and accuracy metrics can be seen in **Table 3** MLP-RF values also MLP-RF with dimensionality reduction technique performed better compare to MLP-RF hybrid approach which is shown in **Figure 8**.

Table 2. Performance parameter comparison.

	Precision (%)	Recall (%)	F-score (%)	Accuracy (%)
MLP	87.8	87.4	87.5	87.3
RF	91.1	91.2	91.1	91.1
MLP-RF	92.6	91.9	91.9	91.8

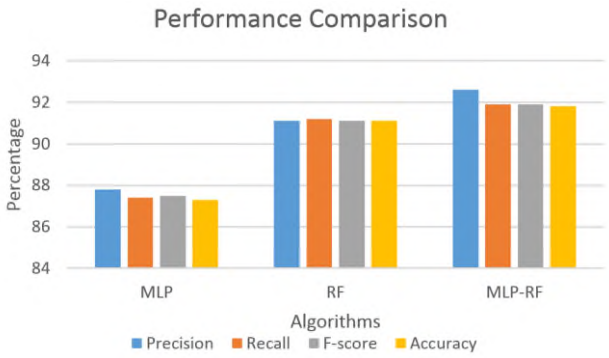

Figure 6. Performance parameters comparison graph.

Table 3. Performance parameter comparison after applying dimensionality reduction algorithm.

	Precision (%)	Recall (%)	F-score (%)	Accuracy (%)
MLP	90.08	90.05	90.05	90.54
RF	93	91.9	91.8	91.89
MLP-RF	96.8	96.8	96.8	96.77

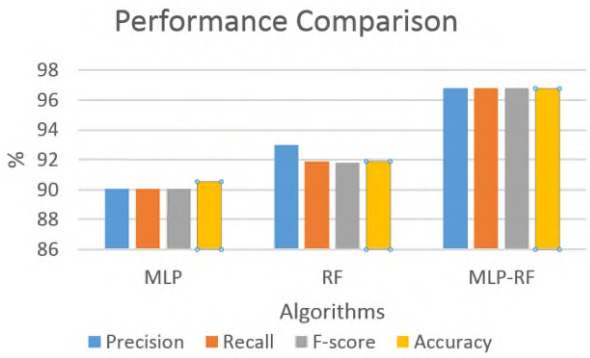

Figure 7. Performance parameters comparison graph.

Following **Figure 8** shows the recall and accuracy comparison of hybrid approach of MLP-RF with hybrid approach of MLP-RF-DR (Dimensionality Reduction).

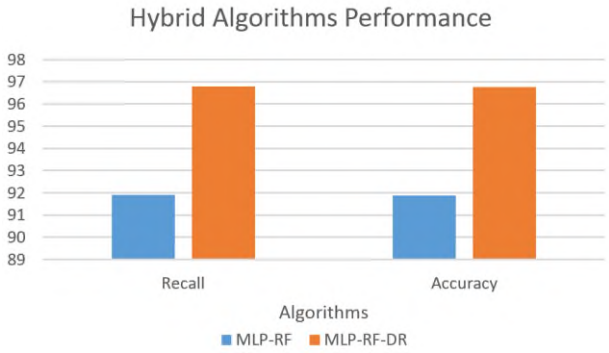

Figure 8. Unsupervised learning workflow.

5. Conclusion

In this study, we employed a sophisticated approach for the multi-stage detection of melanoma. Leveraging the MLP-RF ensemble learning model in conjunction with t-SNE dimensionality reduction, our research yielded compelling results, clearly establishing the superiority of this approach among various machine learning methodologies.

Our experimental findings lead us to the following pivotal conclusions:

1) We implemented a rigorous 10-fold cross-validation strategy for the precise identification of melanoma stages. Remarkably, our MLP-RF-DR model achieved an exceptional recall rate of 96.8% and an accuracy of 96.77%. These outcomes underscore the robustness and efficacy of the MLP-RF-DR model in discerning melanoma stages accurately, holding significant promise for clinical applications.

2) Our comprehensive experimentation and comparative analysis revealed that algorithms incorporating dimensionality reduction consistently outperformed baseline methods such as random forest and multilayer perceptron. Particularly noteworthy, the MLP-RF-DR model exhibited not only a significantly higher recall rate but also superior overall prediction performance when compared to alternative models.

Our study represents a significant advancement in melanoma detection methodology. The MLP-RF-DR model's outstanding performance and the demonstrated advantages of dimensionality reduction techniques open new avenues for enhanced accuracy in melanoma diagnosis. These findings hold substantial implications for the field of dermatology and underscore the potential for further refinement and adaptation of our approach in clinical practice and future research endeavors.

Author contributions

Conceptualization, RA; methodology, RA; validation, DM; formal analysis, MD; writing—original draft preparation, RA; supervision, JRM and SH. All authors have read and agreed to the published version of the manuscript.

Conflict of interest

The authors declare no conflict of interest.

References

1. Skin cancer 101. Available online: http://www.skincancer.org/skin-cancer-information/ (accessed on 23 October 2023).
2. Melanoma overview. Available online: http://www.skincancer.org/skin-cancer-information/melanoma (accessed on 23 October 2023).
3. Vestergaard ME, Macaskill P, Holt PE, Menzies SW. Dermoscopy compared with naked eye examination for the diagnosis of primary melanoma: A meta-analysis of studies performed in a clinical setting. *British Journal of Dermatology* 2008; 159(3): 669–676. doi: 10.1111/j.1365-2133.2008.08713.x
4. Marine A, Walter B. Non-invasive determination of Breslow index. In: Cao MY (editor). *Current Manage Malignant Melanoma*. IntechOpen; 2011. pp. 29–44.
5. Breslow A. Thickness, cross-sectional areas and depth of invasion in the prognosis of cutaneous melanoma. *Annals of Surgery* 1970; 172(5): 902–908. doi: 10.1097/00000658-197011000-00017
6. Marghoob AA, Koenig K, Bittencourt FV, et al. Breslow thickness and clark level in melanoma: Support for including level in pathology reports and in America joint committee on cancer staging. *Cancer* 2000; 88(3): 589–595.
7. Patil R, Bellary S. Machine learning approach in melanoma cancer stage detection. *Journal of King Saud University—Computer and Information Sciences* 2022; 34(6): 3285–3293. doi: 10.1016/j.jksuci.2020.09.002
8. Saez A, Sanchez-Monedero J, Gutierrez PA, Hervas-Martinez C. Machine learning methods for binary and multiclass classification of melanoma thickness from dermoscopic images. *IEEE Transactions on Medical Imaging* 2016; 35(4): 1036–1045. doi: 10.1109/tmi.2015.2506270
9. Rubegni P, Cevenini G, Sbano P, et al. Evaluation of cutaneous melanoma thickness by digital dermoscopy analysis: A retrospective study. *Melanoma Research* 2010; 20(3): 212–217. doi: 10.1097/cmr.0b013e328335a8ff
10. Jaworek-Korjakowska J, Kleczek P, Gorgon M. Melanoma thickness prediction based on convolutional neural network with VGG-19 model transfer learning. In: Proceedings of the 2019 IEEE/CVF Conference on Computer Vision and Pattern Recognition Workshops (CVPRW); 16–17 June 2019; Long Beach, CA, USA. pp. 2748–2756.
11. Naeem A, Farooq MS, Khelifi A, Abid A. Malignant melanoma classification using deep learning: Datasets, performance measurements, challenges and opportunities. *IEEE Access* 2020; 8: 110575–110597. doi: 10.1109/ACCESS.2020.3001507
12. Reshma M, Shan BP. Two methodologies for identification of stages and different types of melanoma detection. In: Proceedings of the 2017 Conference on Emerging Devices and Smart Systems (ICEDSS); 3–4 March 2017; Mallasamudram, India. pp. 257–259.
13. Patil R, Bellary S. Machine learning approach for malignant melanoma classification. *International Journal of Science, Technology, Engineering and Management–A VTU Publication* 2021; 3(1): 40–46.
14. Gaikwad M, Gaikwad P, Jagtap P, et al. Melanoma cancer detection using deep learning. *International Journal of Scientific Research in Science, Engineering and Technology* 2020; 7(3): 394–400. doi: 10.32628/IJSRET
15. Patil R, Bellary S. Transfer learning based system for melanoma type detection. *Revue d'Intelligence Artificielle* 2021; 35(2): 123–130. doi: 10.18280/ria.350203
16. Patil R, Mote A, Mane D. Detection of malignant melanoma using hybrid algorithm. In: Singh P, Singh D, Tiwari V, et al. (editors). *Machine Learning and Computational Intelligence Techniques for Data Engineering*, Proceedings of the MISP 2022: International Conference on Machine Intelligence and Signal Processing; 12–14 March 2022. Springer; 2023. Volume 998, pp. 773–782.
17. Ichim L, Popescu D. Melanoma detection using an objective system based on multiple connected neural networks. *IEEE Access* 2020; 8: 179189–179202. doi: 10.1109/ACCESS.2020.3028248
18. Albahli S, Nida N, Irtaza A, et al. Melanoma lesion detection and segmentation using YOLOv4-DarkNet and active contour. *IEEE Access* 2020; 8: 198403–198414. doi: 10.1109/ACCESS.2020.3035345
19. Zhang N, Cai YX, Wang YY, et al. Skin cancer diagnosis based on optimized convolutional neural network. *Artificial Intelligence in Medicine* 2020; 102: 101756. doi: 10.1016/j.artmed.2019.101756
20. Kassem MA, Hosny KM, Fouad MM. Skin lesions classification into eight classes for ISIC 2019 using deep convolutional neural network and transfer learning. *IEEE Access* 2020; 8: 114822–114832. doi: 10.1109/ACCESS.2020.3003890

21. Cirrincione G, Cannata S, Cicceri G, et al. Transformer-based approach to melanoma detection. *Sensors* 2023; 23(12): 5677. doi: 10.3390/s23125677